Poly(olefin ketone)s: Comparison of the Effects of CH_3 and CH_3CH_2 Side Groups on the Crystal Structure

A. J. Waddon* and N. R. Karttunen

Department of Polymer Science & Engineering, University of Massachusetts, Amherst, Massachusetts 01003

Received September 14, 2000; Revised Manuscript Received February 18, 2002

ABSTRACT: Polyolefin ketone terpolymers with various concentrations of CH_3 and CH_2CH_3 side groups crystallize with inclusion of substituents in the lattice. The degree of crystallinity falls with side group content in both cases and is lower for materials substituted with the larger CH_2CH_3 unit. Using considerations of lattice distortion, melting point depression, and changes in the crystal−amorphous interface (assessed by the broadening of the SAXS long period) as criteria, the point at which the lattice begins to exclude side groups was investigated.

Introduction

Nominally random substituted poly(olefin ketone)s are a class of crystalline olefins with the following structure:

$$[CH_2CH_2C{=}O]_n[CH_2CHRC{=}O]_m$$

For the purposes of this paper R = CH_3 or CH_2CH_3. This paper examines the effect on the crystal structure of both the size of substituent groups and the degree of substitution. In the unsubstituted (R = H) material, crystallization results in a very compact, chain extended orthorhombic crystal of the following dimensions: a = 6.91 Å, b = 5.12 Å, and c = 7.60 Å,[1] the α phase. Upon heating, this material undergoes a solid−solid transition to a slightly expanded cell, the β structure.[2,3] The β structure is also chain extended and orthorhombic with the following dimensions: a = 7.97 Å, b = 4.76 Å, and c = 7.57 Å.[4]

The most obvious effect of even modest levels of CH_3 substitution is to force the room temperature crystal structure to form the β rather than the α cell.[2,5] Lagaron et al.[5] reported that, in the series of materials available to them, at greater than 5.8 mol % substitution, the crystal material was exclusively β.[6] There are also a number of studies[7−9] that have found that the quantity of the higher density α crystals is increased by drawing and orientation.

Previously, by consideration of the reported melting points of various samples sets, we concluded that, in the case of CH_3-substituted materials, these substituent groups were incorporated within the crystalline lattice, at least at relatively low mole fractions.[9] There have also been reports that the CH_3-containing β lattice expands anisotropically along one direction (parallel to a) with substitution, while b and c remain constant,[2,5] rather like the case of substituted polyethylenes.[10] The purpose of this paper is to (a) to consider further the case of CH_3 substitution and (b) expand the previous work to include polymers containing a longer side group (R = CH_2CH_3).

Materials

In this work we compare the structural characteristics of CH_3- and CH_2CH_3-substituted materials. The level of substitution was between 2.0 and 14.6 mol % in the former case and 4.4 and 12.0 mol % in the latter case; exact substitution levels of all samples are shown in Table 1. These were kindly provided by BP-Amoco Chemicals, Grangemouth, UK, in the form of compression-molded sheets of thickness ∼170 μm molded about 20 °C above the melting point and subsequently cooled. The rate of cooling over the main crystallization range was estimated to be approximately 15 °C/min. It is noted that the materials used by Lagaron et al.[5] were reported to be from the same source as ours.

Table 1. Substituent Content of Materials[a]

CH_3 content (mol %)	CH_2CH_3 content (mol %)
2.0	4.4
6.6	5.8
8.8	7.6
10.0	10.0
14.6	12.0

[a] Values expressed as percent of olefin monomers containing side groups as determined by proton NMR. See ref 6 for details of calculation.

Experimental Section

Materials were examined with respect to crystal polymorph and lattice distortion by wide-angle X-ray diffraction (WAXD), the nature of the overlaying lamellar structure by small-angle X-ray scattering (SAXS), and effects on melting behavior and melting point by differential scanning calorimetry (DSC).

WAXD. Diffractometry was carried out with a Siemens D500 operating in normal/transmission mode (0.3° incident slit beam divergence) with Cu Kα radiation and a Ni filter. Experiments were carried out with the incident beam both normal and parallel to the plane of the film.

SAXS. A Rigaku pinhole SAXS camera was used with a Rigaku rotating anode source and Ni-filtered Cu Kα radiation. A Bruker multiwire "Hi-Star" two-dimensional detector was used. The beam was normal to the plane of the sheets.

DSC. Calorimetry was performed with a Du Pont DSC 2910. Samples of approximately 7 mg were heated at a scan rate of 10 °C/min. Values of crystallinity were calculated on the basis of a heat of fusion, ΔH_f, of 227 J/g for the 100% crystalline, unsubstituted material.[11]

Results

WAXD. Parts a and b of Figure 1 show diffractograms of the CH_3-substituted materials in the two projections,

10.1021/ma001589p CCC: $22.00
Published on Web 04/16/2002

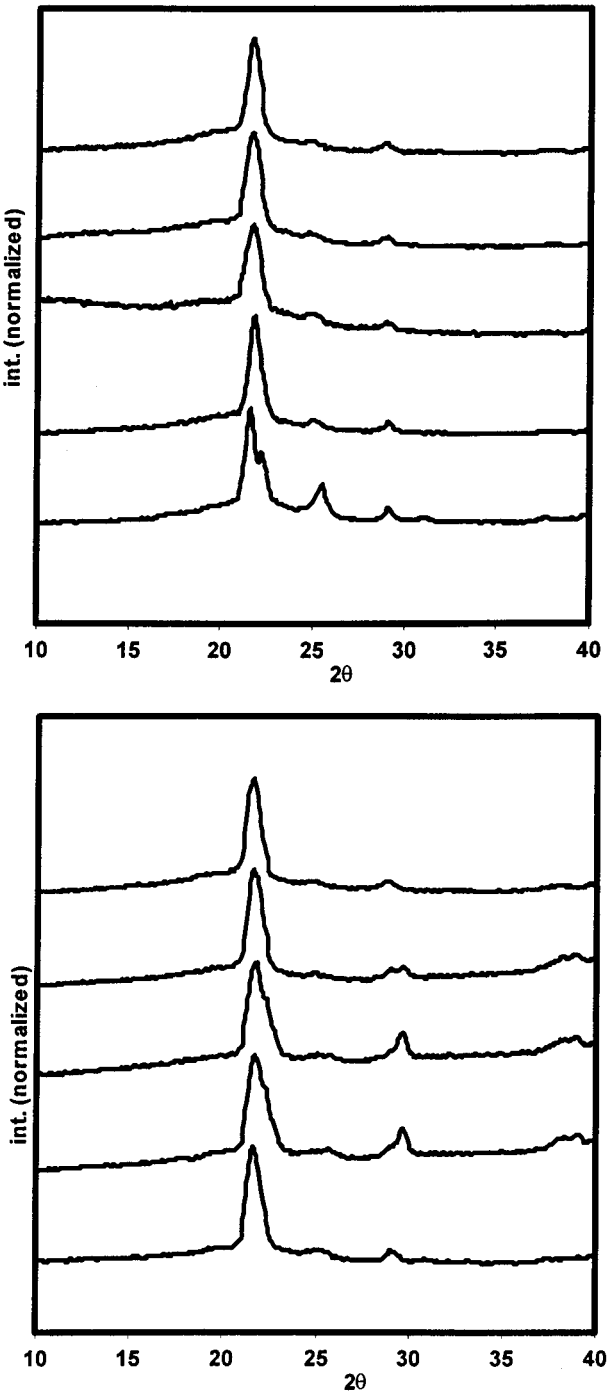

Figure 1. Diffractograms of CH_3 series: beam (a) edge-on and (b) normal. From bottom to top: 2.0, 6.6, 8.8, 10.0, and 14.6 mol %.

edge-on and normal, respectively. This reveals details not readily apparent in an earlier examination.[7]

In edge-on projection, the material of lowest CH_3 content shows two peaks at ~22° and peaks at 25.5°, 29.2°, and 31.1° (Figure 1a). The reflection at 31.1° can be unambiguously identified as the 210 of the α phase, while the reflection at slightly lower angle of 29.2° is 210_β.[2,5] The presence of α phase, as evidenced by 210_α, also suggests that the intense peak at 25.5° is the 200_α rather than the 111_β (which occurs at a somewhat similar angle of 24.8°and therefore overlaps with 200_α). In the 22° range a clearly separate reflection emerges at a higher angle from the main peak of mixed 110_β/110_α. This higher angle peak can be indexed as 200_β. At higher CH_3 contents two points are noted: (a) the evidence for 210_α and 200_α becomes weaker, and (b) 200_β merges with the main peak, appearing first as a shoulder and eventually merging completely. Figure 1b shows that there are slight differences between the projections, indicating subtle orientation effects with $(100)_\beta$ preferentially lying parallel to the film surface. These effects were not investigated further.

In the case of the CH_2CH_3 series, at the lowest substituent content of 4.4 mol %, the splitting of reflections in the 22° range again indicates some difference in spacing between the 110_β and 200_β, Figure 2a. As before, with increasing CH_2CH_3 content, the two peaks at ~22° merge. Comparison with Figure 2b again shows a tendency for $(100)_\beta$ to lie within the plane of the film. Only minimal amounts of α phase material were found in this series.

SAXS. The SAXS profiles for the CH_3 and CH_2CH_3 sets of materials are shown in parts a and b of Figure 3, respectively. The data are shown in the form of Is^2 vs s, where I is intensity and $s = 2(\sin\theta)/\lambda$. Presenting the data in this way shows a maximum corresponding to $s = 0.0083$ Å^{-1} (~120 Å) for both series which moves to slightly larger s with substituent content. The full width at half-maximum (fwhm) of the peaks in Figure 3 has been used as an indication of the peak broadness and has been plotted against substituent content in Figure 4. It can be seen that the maxima in the CH_2CH_3 series are substantially wider than in the CH_3 series. In both cases the maxima become broader with increase in substituent content. Also, in both cases the fwhm approaches a limiting value at higher content (very approximately 10 mol %). There is also a suggestion that at lower concentrations the lines converge.

Melting Points. Figure 5 shows the DSC heating curves for CH_3 materials at 10 °C/min. These show two closely separated melting peaks. Both the melting points (T_m) and heats of fusion decrease with increasing CH_3 content. The appearance of two peaks can represent either two original lamellar populations or reorganization of the lower peak (as found in material crystallized on melt quenching[9]). To investigate this further, one of the materials (14.6 mol %) was scanned at different rates (0.5, 2, 5, and 10 °C/min). The results are shown in Figure 6. In all cases the high-temperature shoulder/peak is evident, suggesting that in this case the dual melting point is due to a second crystal population in the initial material. This is likely to be a result of crystallizing during steady cooling (~15 °C/min), one population crystallizing first and the other later (e.g., as reported elsewhere[12]).

Figure 7 shows the DSC traces for the CH_2CH_3 materials (10 °C/min heating rate). These all show two melting endotherms, also. On scanning the material with 4.4 mol % CH_2CH_3 content (i.e., that most likely to show reorganization) at different rates, it was concluded that these dual melting peaks were also due to a bimodal crystal population in the original material. Again, both the melting points and heats of fusion fall with increasing side-group content.

Figure 8 shows crystallinities (from heats of fusion) for both series. It is noted that the crystallinities for the CH_2CH_3 series are systematically lower than for the CH_3 series. Figure 9 shows the lower and upper melting peak temperatures for both series plus literature values for 0% substitution, plotted against substituent content.

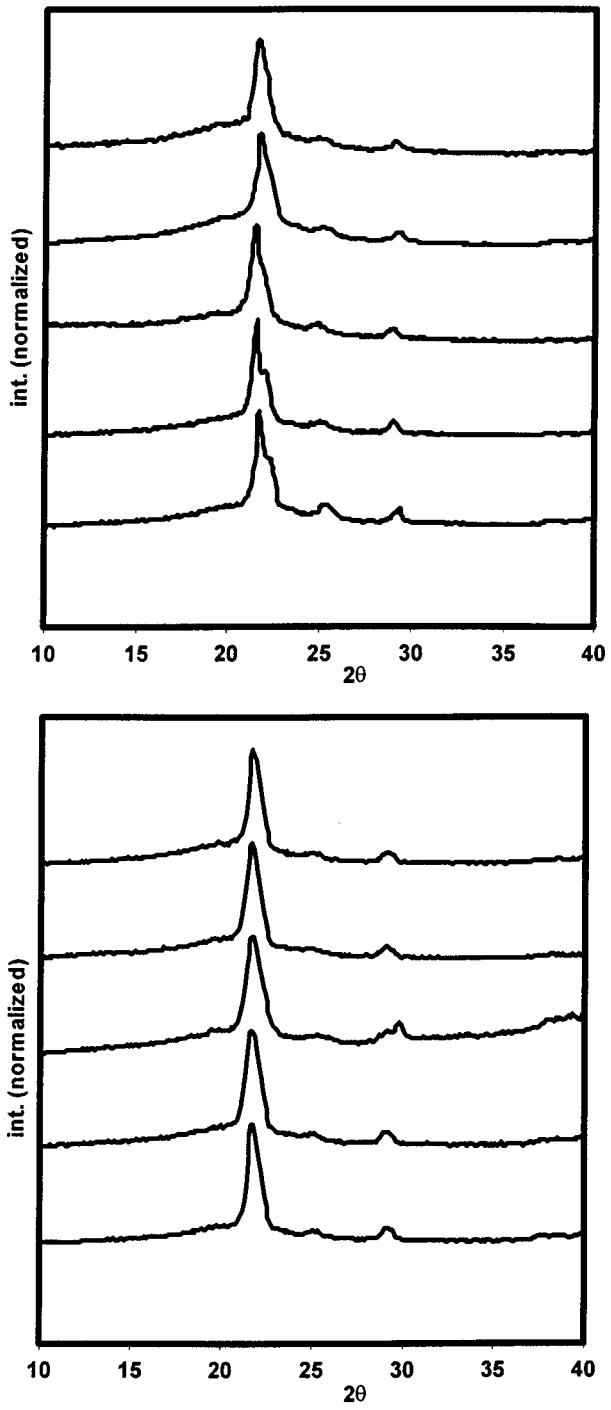

Figure 2. Diffractograms of CH_2CH_3 series: beam (a) edge-on and (b) normal. From bottom to top: 4.4, 5.8, 7.6, 10.0, and 12.0 mol %.

It can be seen that the T_m values for CH_2CH_3-containing materials are systematically lower than for CH_3-containing materials. Also, at low CH_2CH_3 levels, the rate of decrease in melting point is significantly faster than at higher levels.

We have taken our data for this CH_3 series and compiled them with previous literature data for CH_3-substituted polyolefin ketones[2,5,7,9,13,14] (Figure 10). There are clearly differences between data sets, possibly reflecting differences between molecular architecture in sample sets. Nevertheless, the overall trend is still that the rate of decrease in T_m is steeper at low CH_3 concentrations.

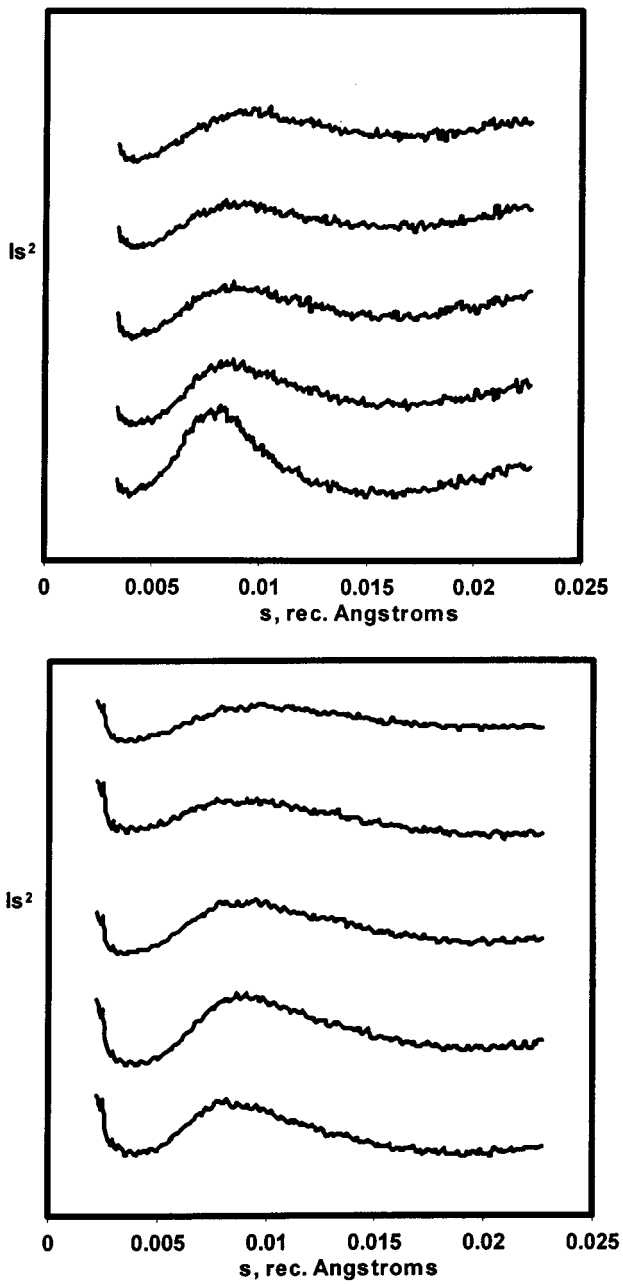

Figure 3. SAXS profiles of (a) CH_3 series (from bottom to top: 2.0, 6.6, 8.8, 10.0, and 14.6 mol %) and (b) CH_2CH_3 series (from bottom to top: 4.4, 5.8, 7.6, 10.0, and 12.0 mol %).

Discussion

It is noted that, in CH_3 materials, definite evidence of the α phase was only seen in the sample of lowest (2.0 mol %) substituent content. Structurally, the incorporation of side groups into the chain forces the α phase to adopt the expanded β phase (17.7 Å^2/chain cross sectional area compared with 19.0 Å^2/chain). Clearly, the reason for this is to accommodate these side groups. While in principle this accommodation may be either inside the lattice or on the lamellar surface, there is evidence showing that methyl groups, at least, can be included within the β lattice.[2,9] The resulting β phase adopts near hexagonal symmetry in which 200 and 110 occur at very similar spacings (as opposed to the α cell where the spacings of 110 and 200 are very different). Reports from other workers indicate that, with increasing amounts of CH_3 side unit, b_β remains constant at

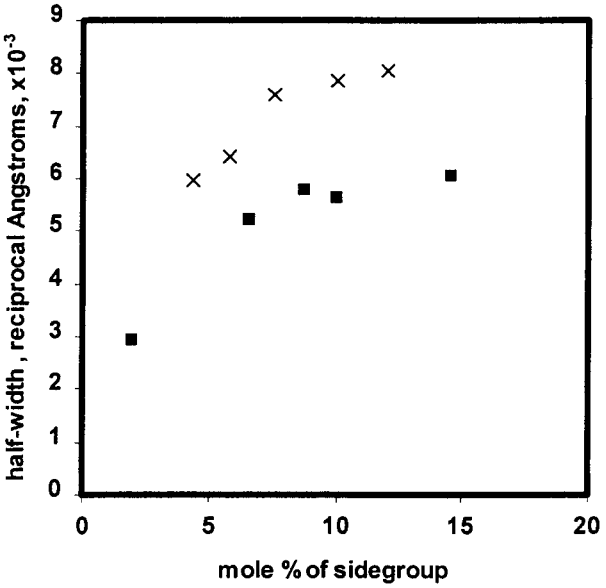

Figure 4. Fwhm of SAXS peaks: CH_3(■), CH_2CH_3 (×).

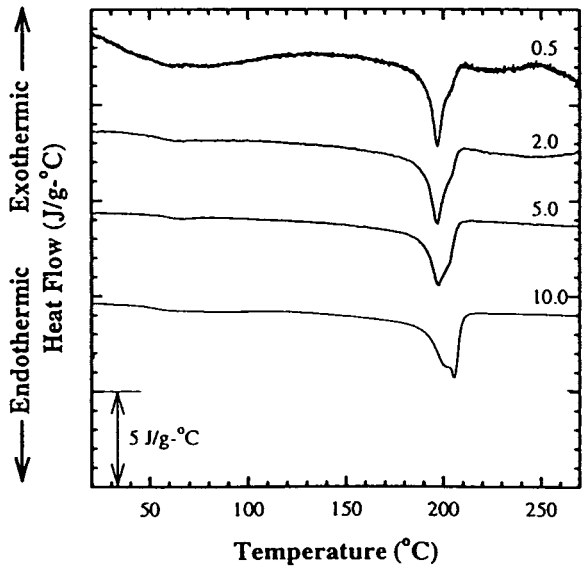

Figure 6. DSC heating scans of CH_3 material of 14.6 mol %; at 0.5, 2, 5, and 10 °C/min.

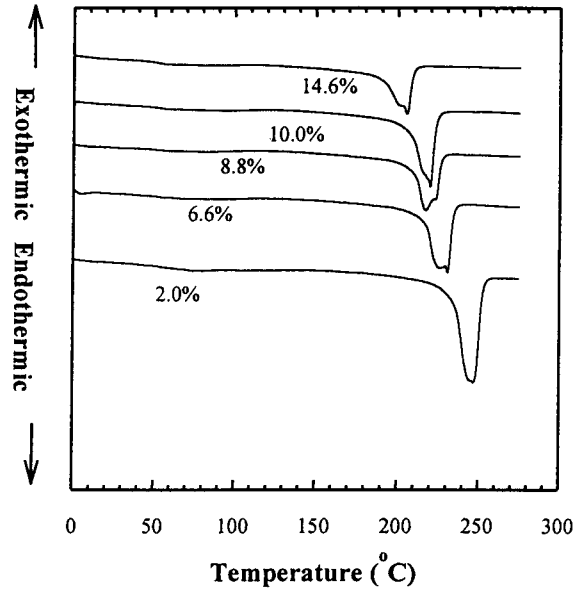

Figure 5. DSC heating scans for CH_3 series at 10 °C/min. From bottom to top: 2.0, 6.6, 8.8, 10.0, and 14.6 mol %.

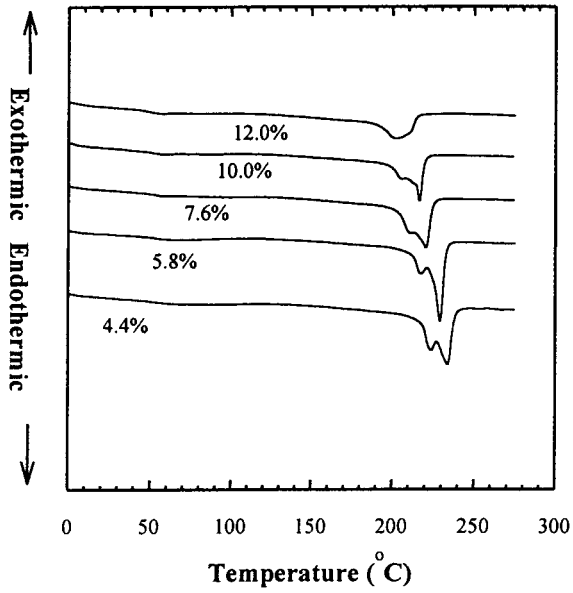

Figure 7. DSC heating scans for CH_2CH_3 series at 10 °C/min. From bottom to top: 4.4, 5.8, 7.6, 10.0, and 12.0 mol %.

4.75 Å while a_β increases[2,5] (in the same way that, in the structurally similar polyethylene, a_{PE} increases with increasing methyl levels while b_{PE} is essentially constant[10]). Our own results show that 110_β and 200_β reflections are well separated at low substituent levels, while at higher levels, 200_β moves to lower angle, gradually merging with 110. This is consistent with anisotropic expansion along a_β with b_β remaining constant since such distortion will affect d_{200} more than d_{110}, thereby leading to peak merger.

In Figure 11 we show the data of Klop et al.[2] and Lagaron et al.[5] for the expansion of a_β as a function of CH_3 content for samples from different sources. There are significant differences in the data. Klop's increase and reach a plateau value of ~8.25 Å, suggesting that the maximum content of CH_3 has been accommodated in the lattice at this point, while Lagaron's show a gradual increase, but always remaining lower than Klop's. This implies a difference in molecular architecture between Klop's set and Lagaron's and, therefore, by implication, ours (since our materials originated from a similar source as Lagaron's).

Such differences in molecular architecture are also suggested by melting points (Figure 10). According to strict predictions of the inclusion model, the fall in T_m with mole percent substituent will be linear as a result of the additional enthalpy of incorporating the substituent within the lattice.[16] The limit of this linearity will be the point at which the lattice is unable to accommodate further inclusions. Beyond this any additional substituted units will be segregated to the noncrystalline regions, causing a consequent entropy loss. It is this entropy loss which is responsible for any further decrease in melting point. Taken alone, our melting point results for CH_3 show a progressive, approximately linear decrease, over the whole range of CH_3 content available, as do those of Lagaron et al.[5] for materials from the same source. However, combining our results with data

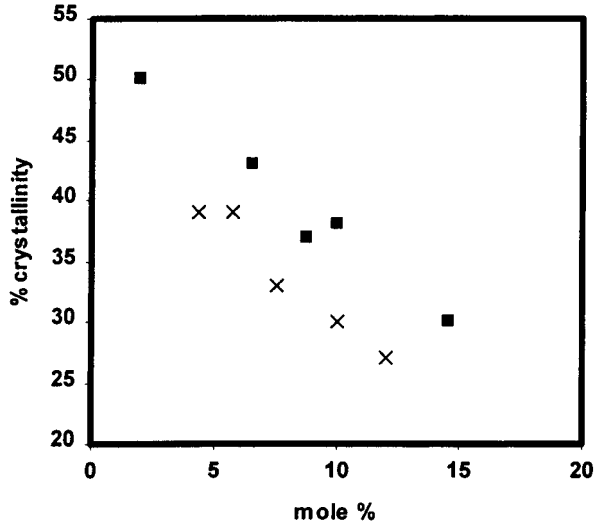

Figure 8. Crystallinities calculated from heats of fusion: CH_3(■), CH_2CH_3 (×).

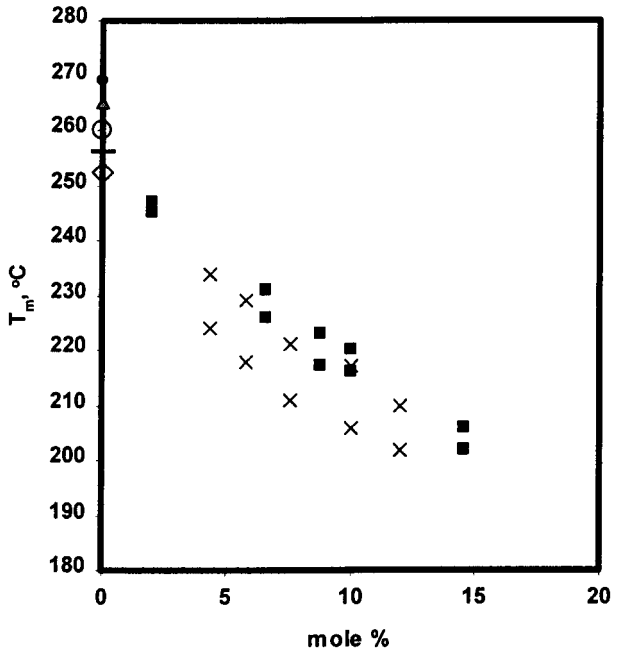

Figure 9. Melting points of CH_3- and CH_2CH_3-substituted materials; upper and lower peak temperatures shown. CH_3 (■), CH_2CH_3 (×). Data for 0% substitution from Klop[2] (●), Lagaron[5] (◇), Waddon[7] (—), Garbassi[13] (▲), and Ash[14] (○).

sets from all available sources shows a trend for curvature in the T_m vs mole fraction relationship (Figure 10). Such curvature is indicative of exclusion of side units at higher mole fractions. There are also important differences in data from varying sources, suggesting differences between nominally identical materials. This reemphasizes the point made by Alamo[15] that small changes in sequence distribution have a significant effect on melting temperatures. We also note that agreement is worse at higher concentrations.

While it is by no means obvious that the larger CH_2CH_3 units can also be included in the lattice, this series shows similar behavior both in crystal polymorph adopted, with the crystal clearly favoring the β modification, and in the progressive distortion of the β lattice toward a near hexagonal structure with increasing levels of CH_2CH_3. It is also noted that the fall in T_m is steeper at low concentrations than at high (Figure 9).

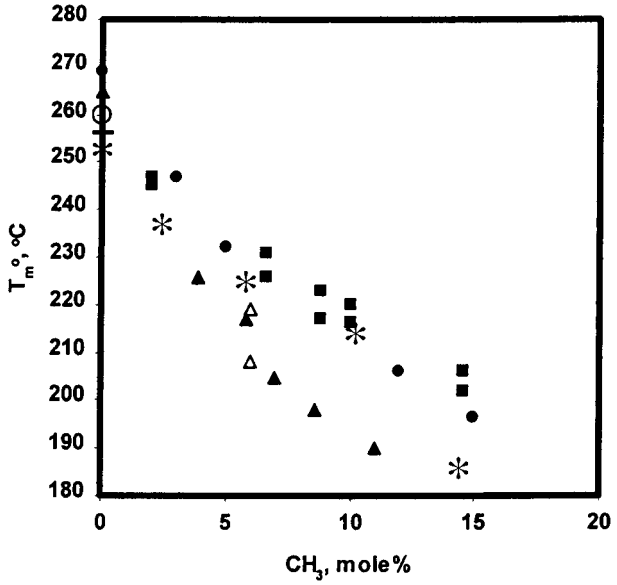

Figure 10. Melting points of various sets of CH_3-substituted materials. Present data (■) (upper and lower melting points). Data also taken from Klop[2] (●), Lagaron[5] (*), Waddon[9] (△), Waddon[7] (—), Garbassi[13] (▲), and Ash[14] (○).

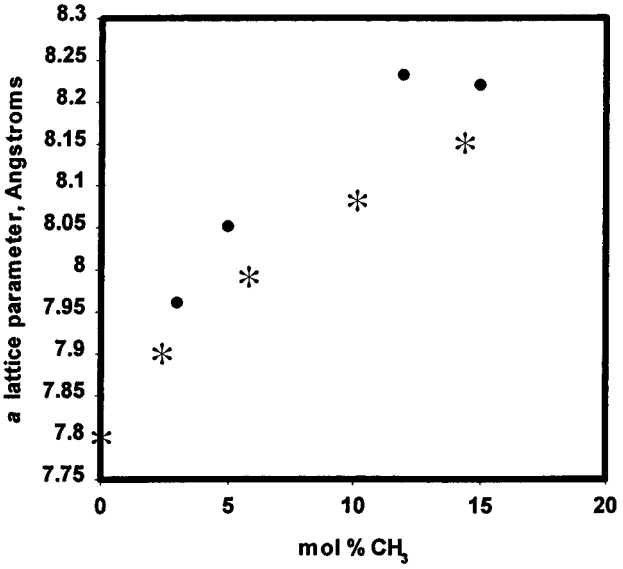

Figure 11. β lattice a parameter of CH_3-substituted materials: data from Klop[2] (●) and Lagaron[5] (*).

This is considered to suggest side group inclusion at low concentrations changing to progressively greater exclusion at higher concentrations.

On direct comparison of the thermal behavior of our CH_3 and CH_2CH_3 series, our results show that the values of T_m and crystallinity (X_c) for the CH_2CH_3 series are consistently lower than for the CH_3 series (Figures 9 and 8, respectively). It is reasonable to attribute this to a larger energy penalty associated with the CH_2CH_3 unit (although it is pointed out that differences in crystallization rates may also lead to lower X_c values for the CH_2CH_3 series).

Turning now to the SAXS results, in both systems, the peaks were sharper at the lowest substituent levels, and the CH_3 series peaks were sharper than the CH_2CH_3 series (Figures 3 and 4). The progressive broadening appears to reach limiting values at ~10 mol %. SAXS broadening can, of course, be caused by the presence of multiple crystal populations of different

thicknesses, which, as the dual melting endotherms indicate, is almost certainly the case here. However, assuming a model of crystalline and amorphous layers separated by an interfacial zone, it is also reasonable to relate the shape of this peak to the profile across this region. As the lattice accommodates greater concentrations of side units, the profile of this interface may be expected to become more irregular. As the crystal composition becomes saturated, the interfacial profile also becomes constant and SAXS broadening from this source plateaus. However, further work is clearly necessary to separate the effects of multiple crystal thicknesses and the nature of the interfacial profile.

Conclusions

It is apparent that at the lowest content of CH_3 (2.0 mol %) some component of the higher density α crystal modification coexists with the majority β phase. Only very trace amounts of α phase appear in the sample with lowest CH_2CH_3 content (4.4 mol %). At higher levels no significant levels of α phase were detected. This is consistent with Lagaron[5] for the case of CH_3-substituted materials provided by the same source as ours.

With the CH_3 series, observations were consistent with inclusion of side units in the β lattice. Similar behavior was also suggested in the CH_2CH_3 series. By considering the scattering angles of the 110_β and 200_β reflections, we found subtle indications of progressive distortion of the β lattice in both series. Also, in both cases, the melting points decreased with side unit content. The lowering of T_m was greater in the CH_2CH_3 case than in the CH_3 case, consistent with a greater disruptive effect on the lattice by CH_2CH_3 groups. Importantly, the rate of fall in T_m decreased at higher CH_2CH_3 levels, consistent with significant exclusion of side units from the lattice at higher CH_2CH_3 content. However, with the present set of CH_3-containing samples, the approach to a limiting value of T_m was not clearly seen, in contrast to results from other CH_3 samples. Finally, SAXS results indicated increasing broadness of the lamellar (long period) reflection with side-group content. This was considered to be possibly attributable to changes in the profile across the crystal-amorphous boundary zone. The fwhm of both series approached a limiting plateau, suggesting a limit in the nature of the interfacial zone with increasing substituent levels.

In both cases, as the substituent level increased, the degree of crystallinity fell. The lowering of crystallinities was clearly greater in the CH_2CH_3 series compared with the CH_3 series, again consistent with the more disruptive effect of including the longer side units.

Importantly, in the case of CH_3-containing materials, comparison with results obtained by other workers on different sample sets showed that materials synthesized by different sources can vary, even though of nominally the same side-group content. As pointed out by Alamo,[15] slight differences in sequence distribution can cause this. This appears to be an issue of some importance, requiring due consideration in such materials.

Acknowledgment. We gratefully acknowledge the support of the NSF funded MRSEC at the University of Massachusetts and also BP-Amoco Chemicals, Grangemouth, UK, for kindly supplying us with material. In particular, we thank Dr. Neil Davidson and Dr. Graham Bonner of BP for their interest in and contribution to this project.

References and Notes

(1) Lommerts, B. J.; Klop, E. A.; Aerts, J. *J. Polym. Sci., Polym. Phys. Ed.* **1993**, *31*, 1319.
(2) Klop, E. A.; Lommerts, B. J.; Veurink, J.; Aerts, J.; van Puijenbroek, R. R. *J. Polym. Sci., Polym. Phys. Ed.* **1995**, *33*, 315.
(3) Wittmann, J. C.; Grayer, V.; Lotz, B.; Smith, P.; Lommerts, B. J. *Polym. Prepr.* **1995**, *36*, 257.
(4) Chatani, Y.; Takizawa, T.; Murahashi, S.; Sakata, Y.; Nishimura, Y. *J. Polym. Sci.* **1961**, *55*, 811.
(5) Lagaron, J. M.; Vickers, M. E.; Powell, A. K.; Davidson, N. S. *Polymer* **2000**, *41*, 3011.
(6) Note that in ref 5 mole fractions of substituents are calculated as a fraction of all monomer units, including C═O units; here the more usual method of expressing the substituent content as a fraction of just the olefin monomers has been followed. These values will therefore be twice the values calculated by the method of ref 5.
(7) Waddon, A. J.; Karttunen, N. R. *Polymer* **2001**, *42*, 2039.
(8) Kalay, G.; Bevis, M. J. *J. Polym. Sci., Polym. Phys. Ed.* **1997**, *35*, 415.
(9) Waddon, A. J.; Karttunen, N. R.; Lesser, A. J. *Macromolecules* **1999**, *32*, 423.
(10) Swan, P. R. *J. Polym. Sci.* **1962**, *56*, 409.
(11) Flood, J. E.; Weinkauf, D. H.; Londa, M. *53rd ANTEC Technol. Conf. Pap.* **1995**, *2*, 2326.
(12) Lu, J.; Li, C. K. Y.; Wei, G. X.; Sue, H. J. *J. Mater. Sci.* **2000**, *35*, 271.
(13) Garbassi, F.; Sommazzi, A.; Meda, L.; Mestroni, G.; Sciutto, A. *Polymer* **1998**, *39*, 1503.
(14) Ash, C. E.; Flood, J. E. *Polym. Mater. Sci. Eng., ACS Conf. Proc.* **1997**, 110.
(15) Alamo, R.; Domszy, R.; Mandelkern, L. *J. Phys. Chem.* **1984**, *88*, 6587.
(16) Sanchez, I. C.; Eby, R. K. *J. Res. Natl. Bur. Stand. (Phys. Chem.)* **1973**, *77A*, 353.

MA001589P